The Kinetics of Cyanide and Fluoride Binding by Ferric Horseradish Peroxidase*

William D. Ellis† and H. Brian Dunford

ABSTRACT: The kinetics of the reversible binding of cyanide by ferric horseradish peroxidase has been studied over the pH range 4.2–11.3 by means of a stopped-flow apparatus. Analysis of the pH dependence of the bimolecular rate constants is consistent with the presence of three heme-linked ionizable groups on peroxidase with pK values of 4.1, 6.4, and 10.8. It is not possible to distinguish whether HCN or CN^- is the attacking species, but the bound form of the ligand appears to be the cyanide ion. The kinetic results obtained for fluoride binding by horseradish peroxidase are reanalyzed, and it is shown that the published mechanism requires extension because it violates the principle of detailed balancing. A satisfactory mechanism for the pH range 4.1–7.9 postulates that fluoride ion binds to peroxidase which contains two heme-linked acid groups with pK values of 4.3 and 6.1. These are in agreement with the results of the cyanide kinetic analysis.

A study of the kinetics of cyanide binding to HRP[1] might be expected to yield fundamental information about the nature of the active site in peroxidase. An early study of this reaction at pH 4.2 and 6.2 showed little change in the value of the forward rate constant (Chance, 1943). We report here on a study of this reaction at 19 values of pH, ranging from 4.21 to 11.31. Kinetic results obtained in a study of fluoride binding by horseradish peroxidase (Dunford and Alberty, 1967) are reexamined and extended by application of the principle of detailed balancing.

Experimental Section

Kinetic measurements were made using a stopped-flow apparatus. A spectrophotometric detection system was used which consisted of a 50-W Ace projection lamp; a Bausch and Lomb Model 33-86-26-07 high-intensity Model 5 grating monochrometer; an R.C.A. Model 1P28 photomultiplier in a circuit with an emitter follower output; and a Tektronix 535A oscilloscope with a type D high-gain differential plug-in preamplifier. A Hewlett-Packard Harrison Model 6264A dc power supply for the tungsten lamp provided 8 V with 0.01% line and load regulation and 500-μV ripple. Photomultiplier voltage was obtained from a Hewlett-Packard Harrison 6110A dc power supply. Experimental traces were photographed with a 35-mm camera mounted on the oscilloscope with a Beattie-Coleman Polexa adapter. Driving syringes, mixing chamber, and observation tube of the stopped-flow apparatus were all enclosed in a thermostated bath which was kept at 25.0 ± 0.1°. Auxiliary absorbance measurements and spectrophotometric equilibrium constant determinations were made on a Beckman DU spectrophotometer. A Beckman expanded-scale pH meter was used for all pH measurements.

Pure HRP (RZ 2.88, lot no. 6485206) and crude HRP (RZ 0.89) were obtained from Boehringer-Mannheim Corp., New York, N. Y. Reagent grade KCN (Fisher) was used without further purification. The concentrations of stock KCN solutions were determined by titration with a standard silver nitrate solution using potentiometric determination of the end point. Below pH 8, possible loss of HCN was minimized by using solutions of cyanide which were less than 10^{-4} M and by keeping them in tightly closed vessels which contained only a small volume of air. All solutions were made from conductivity water.

Solutions of HRP and cyanide were each made to the desired pH using buffer of ionic strength 0.01 and sufficient potassium nitrate so that the total ionic strength was constant at μ = 0.11. Concentrations of HRP and cyanide were varied at different pH values in such a manner that the experimental absorbances ranged from 0.25 to 0.50, which is in the region of minimum error due to instrumental uncertainty.

The buffer systems employed at various pH ranges were: acetate below pH 5.5, cacodylic acid between pH 5.5 and 7.0, Tris–nitric acid between pH 7.0 and 9.0, borate between pH 8.0 and 10.0, glycine between pH 9.0 and 11.0, and potassium hydroxide above pH 11. Each buffer was checked for possible complexing with HRP by examining the spectrum of HRP at a particular pH in the presence and absence of buffer. In addition, ex-

* From the Department of Chemistry, University of Alberta, Edmonton, Alberta, Canada. *Received November 7, 1967.* Supported financially by the National Research Council.

† Holder of an Izaak Walton Killam Memorial fellowship.

[1] Abbreviations used that are not listed in *Biochemistry 5*, 1445 (1966), are: HRP or P, ferric horseradish peroxidase; RZ, purity number; CN and PCN, all ionizable species of cyanide and complex; HP, H_2P, protonated forms of peroxidase; $(\bar{P})$, $(\bar{CN})$, and $(\bar{PCN})$, equilibrium concentrations of all forms of peroxidase, cyanide, and complex; $(P)_0$ and $(CN)_0$, initial concentrations of all forms of peroxidase and cyanide; K_L, dissociation constant of ligand; K_{diss}, dissociation constant of peroxidase–cyanide complex; k_{1app} and k_{-1app}, apparent second-order binding rate constant and apparent first-order dissociation rate constant.

periments were repeated with two or more different buffers in all overlapping regions. In all cases, experiments at the same pH but with different buffer gave results agreeing within experimental error.

HRP and its complexes are known to undergo splitting at extremes of pH (Maehly, 1952). Experiments at the pH extremes were performed with sufficient rapidity that the decrease in absorbance of HRP at 403 mμ during the experiment was less than 1%. Above pH 10 problems in pH control were encountered because of absorption of carbon dioxide from the atmosphere. These were overcome by using freshly boiled water for solutions and by passing nitrogen over any vessel open to the air during the preparation of solutions.

All absorbance and transmittance measurements from which kinetic and equilibrium parameters were obtained were made using light of wavelength 422 mμ, which corresponds to the maximum of the Soret peak of the HRP–CN complex.

Photographs of the experimental oscilloscope traces provided a record of photomultiplier output voltage *vs.* time. Values of these quantities were read from an enlargement of the picture and the results were converted into concentration of the HRP–CN complex *vs.* time in the following manner. Voltage was converted into total absorbance with the aid of calibrating values obtained from auxiliary absorbance measurements made on the HRP solution and the reaction equilibrium mixture; concentration of the complex was then calculated from total absorbance at 422 mμ using the molar absorptivities of HRP and HRP–CN at that wavelength (Keilin and Hartree, 1951).

Results

The equation for the reaction studied is that for second-order–first-order reversible kinetics.[2]

$$P + CN \underset{k_{-1\,app}}{\overset{k_{1\,app}}{\rightleftharpoons}} PCN \qquad (1)$$

The corresponding differential rate equation is

$$\frac{d(PCN)}{dt} = k_{1\,app}(P)(CN) - k_{-1\,app}(PCN) \qquad (2)$$

The results were analyzed by direct use of eq 2, but with $d(PCN)/dt$ approximated by $\Delta(PCN)/\Delta t$; *i.e.*, by taking a chord over a short interval as equal to the tangent at the center of that interval. Using this approximation, along with the average concentration of PCN complex within the interval, $(PCN)_{av}$, eq 2 becomes

$$\frac{\Delta(PCN)}{\Delta t} = k_{1\,app}[(P)_0 - (PCN)_{av}][(CN)_0 - (PCN)_{av}] - k_{-1\,app}(PCN)_{av} \qquad (3)$$

[2] We use the symbols $\rightleftarrows$ for reactions occurring at measurable rates and $\rightleftharpoons$ for reactions in which equilibrium is assumed to be maintained (King, 1964).

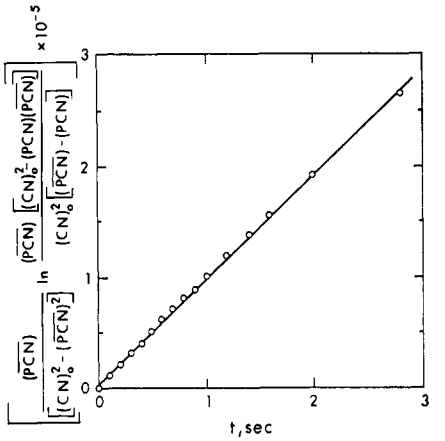

FIGURE 1: Test of reversible second-order–first-order kinetics. The left side of eq 4 is plotted *vs.* time using data for the reaction of HRP with cyanide at pH 6.5. The slope is equal to $k_{1\,app}$.

In order that the chords would be good approximations of tangents, the following technique was used: $\Delta(PCN)/\Delta t$ was determined over short intervals of time in the early stages of the reaction when the rate was changing rapidly with time, and then at increasingly larger intervals as the reaction approached equilibrium. Values of $k_{1\,app}$ and $k_{-1\,app}$ could then be obtained from eq 3 when experimental data consisting of $\Delta(PCN)/\Delta t$ and the corresponding $(PCN)_{av}$ were used with a nonlinear least-squares computer program (IBM Share Library, 1964). Fifteen to twenty points from each experiment were used to help ensure a valid analysis.

Although eq 2 can be integrated when $(P)_0 \neq (CN)_0$, the resultant equation is complex (Ver Ploeg and Alberty, 1968). For the case where $(P)_0 = (CN)_0$, the integrated form of eq 2 is

$$\frac{(\overline{PCN})}{[(CN)_0^2 - (\overline{PCN})^2]} \times \ln \frac{(\overline{PCN})[(CN)_0^2 - (PCN)(\overline{PCN})]}{(CN)_0^2[(\overline{PCN}) - (PCN)]} = k_{1\,app}t \qquad (4)$$

(Frost and Pearson, 1961). A plot of the left side of this equation *vs.* time should give a straight line of slope equal to $k_{1\,app}$ and an intercept of zero. Unfortunately, eq 4 suffers from two disadvantages: it does not yield $k_{-1\,app}$ and it can be used only if $(P)_0$ equals $(CN)_0$. A plot of the left side of eq 4 *vs.* time for an experiment at pH 6.5 where $(P)_0$ was equal to $(CN)_0$ is shown in Figure 1. The resulting value for $k_{1\,app}$ agreed within 5% of the value obtained using the computer analysis of eq 3.

The experimental rate constants obtained at each pH studied are presented in Table I. Also found in that table are values of the dissociation constants for the HRP–CN complex obtained in two different ways: direct spectrophotometric determination and calculation from $K_{diss} = k_{-1\,app}/k_{1\,app}$. The spectrophotometric determination consisted of determining $(\overline{PCN})$ for an equilibrium mixture of HRP and cyanide and using eq 5 for calculation of the equilibrium constant. Plots of the logs of $k_{1\,app}$,

TABLE I: Data for the Binding of Cyanide by Peroxidase at 25°.

pH	Exptl Rate Constants with Std Dev		$K_{diss} = \frac{(P)(\overline{CN})}{(\overline{PCN})}$	
	k_{1app} (M^{-1} sec^{-1})	k_{-1app} (sec^{-1})	From Kinetic Data	Spectrophotometric Detn[a]
4.21	$(6.1 \pm 0.3) \times 10^4$	$(1.7 \pm 0.2) \times 10^{-1}$	$(2.9 \pm 0.4) \times 10^{-6}$	$(2.6 \pm 0.2) \times 10^{-6}$
4.46	$(7.3 \pm 0.3) \times 10^4$	$(1.7 \pm 0.2) \times 10^{-1}$	$(2.3 \pm 0.3) \times 10^{-6}$	2.1×10^{-6}
4.96	$(8.8 \pm 0.5) \times 10^4$	$(1.9 \pm 0.2) \times 10^{-1}$	$(2.1 \pm 0.3) \times 10^{-6}$	2.0×10^{-6}
5.50	$(1.2 \pm 0.1) \times 10^5$	$(1.9 \pm 0.2) \times 10^{-1}$	$(1.7 \pm 0.3) \times 10^{-6}$	$(1.5 \pm 0.2) \times 10^{-6}$
5.94	$(1.0 \pm 0.1) \times 10^5$	$(1.8 \pm 0.3) \times 10^{-1}$	$(1.7 \pm 0.3) \times 10^{-6}$	1.6×10^{-6}
6.50	$(9.7 \pm 0.5) \times 10^4$	$(2.0 \pm 0.2) \times 10^{-1}$	$(2.1 \pm 0.2) \times 10^{-6}$	$(1.9 \pm 0.2) \times 10^{-6}$
7.05	$(9.8 \pm 0.5) \times 10^4$	$(2.8 \pm 0.3) \times 10^{-1}$	$(2.9 \pm 0.3) \times 10^{-6}$	$(2.4 \pm 0.2) \times 10^{-6}$
7.47	$(9.0 \pm 0.5) \times 10^4$	$(2.9 \pm 0.3) \times 10^{-1}$	$(3.2 \pm 0.4) \times 10^{-6}$	2.7×10^{-6}
8.11	$(7.2 \pm 0.4) \times 10^4$	$(2.9 \pm 0.3) \times 10^{-1}$	$(4.1 \pm 0.5) \times 10^{-6}$	$(3.5 \pm 0.1) \times 10^{-6}$
8.55	$(6.6 \pm 0.4) \times 10^4$	$(2.9 \pm 0.2) \times 10^{-1}$	$(4.3 \pm 0.4) \times 10^{-6}$	$(4.0 \pm 0.2) \times 10^{-6}$
8.98	$(4.6 \pm 0.3) \times 10^4$	$(3.2 \pm 0.2) \times 10^{-1}$	$(7.0 \pm 0.5) \times 10^{-6}$	$(6.3 \pm 0.5) \times 10^{-6}$
9.39	$(2.4 \pm 0.2) \times 10^4$	$(2.9 \pm 0.2) \times 10^{-1}$	$(1.2 \pm 0.1) \times 10^{-5}$	$(1.2 \pm 0.1) \times 10^{-5}$
9.84	$(1.0 \pm 0.1) \times 10^4$	$(2.3 \pm 0.1) \times 10^{-1}$	$(2.3 \pm 0.1) \times 10^{-5}$	2.2×10^{-5}
10.10	$(5.9 \pm 1.1) \times 10^3$	$(2.6 \pm 0.3) \times 10^{-1}$	$(4.5 \pm 0.7) \times 10^{-5}$	$(4.2 \pm 0.7) \times 10^{-5}$
10.33	$(3.4 \pm 0.3) \times 10^3$	$(1.9 \pm 0.2) \times 10^{-1}$	$(5.7 \pm 0.6) \times 10^{-5}$	5.4×10^{-5}
10.48	$(2.2 \pm 0.2) \times 10^3$	$(2.0 \pm 0.2) \times 10^{-1}$	$(9.1 \pm 1.4) \times 10^{-5}$	$(8.8 \pm 0.4) \times 10^{-5}$
10.73	$(1.0 \pm 0.1) \times 10^3$	$(1.3 \pm 0.1) \times 10^{-1}$	$(1.3 \pm 0.2) \times 10^{-4}$	$(1.3 \pm 0.1) \times 10^{-4}$
11.05	$(2.7 \pm 0.3) \times 10^2$	$(8.9 \pm 1.2) \times 10^{-2}$	$(3.3 \pm 0.6) \times 10^{-4}$	$(3.1 \pm 0.4) \times 10^{-4}$
11.31	$(1.0 \pm 0.1) \times 10^2$	$(7.3 \pm 1.0) \times 10^{-2}$	$(7.1 \pm 1.2) \times 10^{-4}$	6.6×10^{-4}

[a] Error limits are average deviations for multiple determinations; no limits given for single determinations.

$$K_{diss} = \frac{[(P)_0 - (\overline{PCN})][(CN)_0 - (\overline{PCN})]}{(\overline{PCN})} \quad (5)$$

k_{-1app}, and K_{diss} *vs.* pH are shown in Figures 2–4, respectively.

Most of the work was done using crude HRP; runs at pH 4.2, 5.5, and 8.5 were repeated using pure HRP. The results obtained from the pure HRP agreed within 10% of the corresponding results using crude HRP. As will be discussed further in a future publication, the possible presence of isozymes in the crude commercial HRP is not expected to affect appreciably the kinetic results or their interpetation (Shannon *et al.*, 1966; Kay *et al.*, 1967).

Discussion

The pK for the dissociation of hydrocyanic acid is 9.21 at 25° and 0 μ (Izatt *et al.*, 1962). An extended Debye–Hückel equation (Davies, 1938) was used to calculate the activity coefficients at $\mu = 0.11$ and yielded a corrected pK of 9.0. Since the study was made over a pH range encompassing both sides of this pK, both CN^- and HCN must be considered as possible binding ligands. The first mechanism considered is the binding of cyanide to HRP with no heme-linked ionizable groups.[3]

[3] We define a heme-linked ionizable group as any ionizable group in HRP which influences the binding of a ligand at the sixth coordination position of the heme ferric iron. This group may be part of either the prosthetic group or the protein moiety.

$$\begin{array}{ccc} CN^- + P & \xrightarrow{k_1} & PL \\ {\scriptstyle K_L}\uparrow\downarrow & & \\ HCN + P & \xrightarrow{k_2} & PL \end{array} \quad (I)$$

The representation of mechanism I contains two simplifying features: hydrogen ions have been omitted and the HRP–ligand complex has been designated PL without specifying whether the ligand is bound as HCN or CN^- since this is irrelevant to the analysis of the k_{1app} data. The form of the complex and the nature of the reverse reaction will be considered for the analysis of the k_{-1app} data. From mechanism I

$$k_{1app} = \frac{k_1}{\left(1 + \frac{(H^+)}{K_L}\right)} + \frac{k_2}{\left(1 + \frac{K_L}{(H^+)}\right)} \quad (6)$$

Equation 6 can be rearranged to the form of a linear equation

$$k_{1app}\left(1 + \frac{K_L}{(H^+)}\right) = k_2 + \frac{k_1 K_L}{(H^+)} \quad (7)$$

If mechanism I were valid, a plot of $k_{1app}(1 + K_L/(H^+))$ *vs.* $1/(H^+)$ would be linear, with a slope equal to k_1K_L and an intercept equal to k_2. As can be seen in Figure 5, this plot is not linear, so mechanism I is not valid.

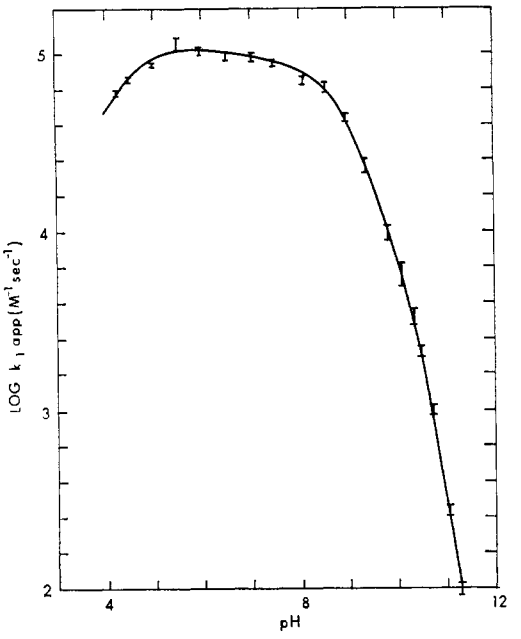

FIGURE 2: Plot of log $k_{1\,app}$ *vs.* pH for the binding of cyanide by HRP. The solid line is calculated using the best-fit parameters of mechanism V.

The next simplest mechanism (mechanism II) involves the participation of one heme-linked group. Total

$$\begin{array}{ccc} \mathrm{HP} & \left\{\begin{array}{l} +\ \mathrm{CN^-} \xrightarrow{k_3} \\ +\ \mathrm{HCN} \xrightarrow{k_4} \end{array}\right\} & \mathrm{HPL} \\ K_1 \uparrow\downarrow & & \\ \mathrm{P} & \left\{\begin{array}{l} +\ \mathrm{CN^-} \xrightarrow{k_5} \\ +\ \mathrm{HCN} \xrightarrow{k_6} \end{array}\right\} & \mathrm{PL} \end{array} \qquad \text{(II)}$$

charges on the peroxidase species and the equilibria involving the ligand species have been omitted, although the effect of the dissociation of HCN on the concentration of ligand has been taken into account in the mathematical treatment of the mechanism. For mechanism II

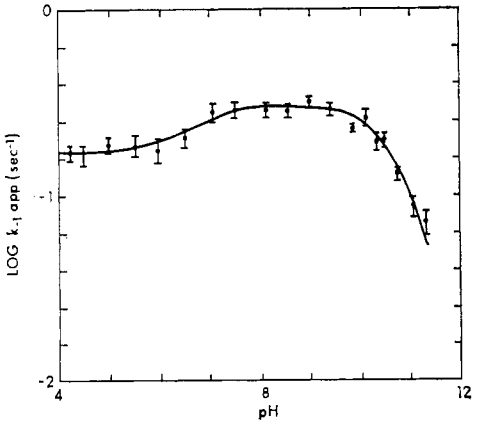

FIGURE 3: Plot of log $k_{-1\,app}$ *vs.* pH for the dissociation of the HRP–cyanide complex. The solid line is calculated using the best-fit parameters of mechanism V.

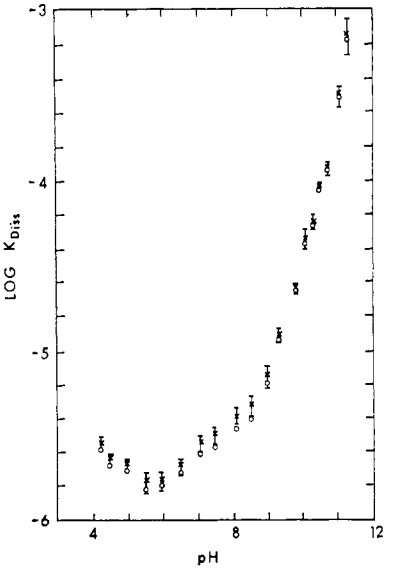

FIGURE 4: Plot of log K_{diss} *vs.* pH for the HRP–CN complex. Crosses with magnitudes of uncertainty were obtained from $k_{-1\,app}/k_{1\,app}$ data (Table I). Circles represent values obtained from direct spectrophotometric measurements.

$$k_{1app} = \frac{k_3 + \dfrac{k_4(\mathrm{H^+})}{K_L} + \dfrac{k_5 K_1}{(\mathrm{H^+})} + \dfrac{k_6 K_1}{K_L}}{1 + \dfrac{K_1}{(\mathrm{H^+})} + \dfrac{(\mathrm{H^+})}{K_L} + \dfrac{K_1}{K_L}} \qquad (8)$$

Equation 8 can be used with a nonlinear least-squares program (IBM Share Library, 1964) to yield the best-fit values of specific rate constants and equilibrium constant for the heme-linked group. Because the $k_{1\,app}$ values have a range of 10^3, the nonlinear least-squares program was modified for these and all subsequent analyses to minimize the sum of the squares of the relative residuals rather than the sum of the squares of the absolute residuals. If k_3 and k_5 are set equal to zero, eq 8 represents a mechanism where HCN is postulated to be the only effective attacking ligand, and if k_4 and k_6 are set equal to zero it represents CN^- as the only effective at-

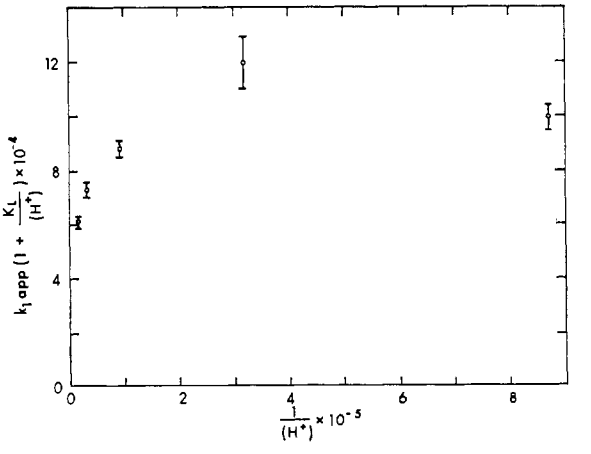

FIGURE 5: Test of mechanism for HCN and CN^- binding to peroxidase with no heme-linked acid groups (mechanism I). If this mechanism were valid the plot of $k_{1\,app}(1 + K_L/(H^+))$ *vs.* $1/(H^+)$ would be linear.

TABLE II: Rate and Equilibrium Constants Obtained from Analysis of Eq 9 and 10.

Mechanism III, Eq 9	Mechanism IV, Eq 10
$k_7 = (1.0 \pm 0.1) \times 10^{10}$ M^{-1} sec^{-1}	$0 \leq k_9 \leq 1 \times 10^4$ M^{-1} sec^{-1}
$0 \leq k_8 \leq 20$ M^{-1} sec^{-1}	$k_{10} = (9.6 \pm 0.7) \times 10^4$ M^{-1} sec^{-1}
$K_2 = (1.1 \pm 0.1) \times 10^{-4}$ M	$K_2 = (1.1 \pm 0.1) \times 10^{-4}$ M
$K_3 = (1.5 \pm 0.4) \times 10^{-11}$ M	$K_3 = (1.5 \pm 0.4) \times 10^{-11}$ M

tacking ligand. Although all combinations were tried using nonlinear least-squares analysis, it was not possible to fit the $k_{1\,app}$ data within experimental error. Thus mechanism II is eliminated.

The next mechanisms to consider involve two heme-linked ionizable groups. A large number of possible combinations of attacking ligands and bound ligands can be conceived for such a mechanism. We will discuss briefly only two of those possibilities, the only two which came close to fitting the experimental rate data using nonlinear least-squares analysis.

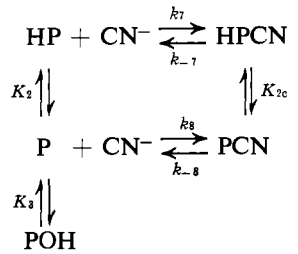

(III)

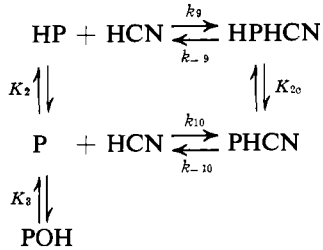

(IV)

From these mechanisms, one can write eq 9–12.

$$k_{1\,app}\left(1 + \frac{(H^+)}{K_L}\right) = \frac{k_7}{1 + \frac{K_2}{(H^+)} + \frac{K_2K_3}{(H^+)^2}} + \frac{k_8}{1 + \frac{(H^+)}{K_2} + \frac{K_3}{(H^+)}} \quad (9)$$

$$k_{1\,app}\left(1 + \frac{K_L}{(H^+)}\right) = \frac{k_9}{1 + \frac{K_2}{(H^+)} + \frac{K_2K_3}{(H^+)^2}} + \frac{k_{10}}{1 + \frac{(H^+)}{K_2} + \frac{K_3}{(H^+)}} \quad (10)$$

$$k_{-1\,app} = \frac{k_{-7}}{1 + \frac{K_{2c}}{(H^+)}} + \frac{k_{-8}}{1 + \frac{(H^+)}{K_{2c}}} \quad (11)$$

$$k_{-1\,app} = \frac{k_{-9}}{1 + \frac{K_{2c}}{(H^+)}} + \frac{k_{-10}}{1 + \frac{(H^+)}{K_{2c}}} \quad (12)$$

Equations 9 and 11 correspond to mechanism III and eq 10 and 12 correspond to mechanism IV. By proper choice of the values for the adjustable parameters in both eq 9 and 10, a satisfactory fit to the $k_{1\,app}$ data is obtained. The best-fit parameters and their standard deviations obtained from nonlinear least-squares analysis are shown in Table II. The specific rate constants k_8 and k_9 have *effective* values of zero, which means that although they might have finite values, their corresponding terms in eq 9 and 10 do not affect significantly the predicted values of $k_{1\,app}$. They are included, however, because of the discussion below of the principle of detailed balancing. Upper limits on their values, shown in Table II, are estimated by assuming that the corresponding terms in eq 9 and 10 contribute a maximum of 5% to the predicted values of $k_{1\,app}$.

The predicted value of the pK of the most basic heme-linked group, 10.8, appears to correspond to the pK for the formation of the HRP–hydroxide complex. This pK has been measured at values ranging from 10.6 to 11.3 (Harbury, 1957; Theorell, 1942). We therefore have used P and POH in mechanisms III and IV to represent HRP with the most acid heme-linked groups ionized, and with water and hydroxide, respectively, in the sixth coordination position of the heme ferric iron.

One flaw of mechanisms III and IV is that they allow no simple explanation for the behavior of $k_{-1\,app}$ at high pH. For the pH region 4.2–9.4, nonlinear least-squares analyses of eq 11 and 12 give the best-fit parameters and their standard deviations: $k_{-7} \equiv k_{-9} = 0.17 \pm 0.02$ sec^{-1}; $k_{-8} \equiv k_{-10} = 0.30 \pm 0.02$ sec^{-1}, and $K_{2c} = (1.9 \pm 0.8) \times 10^{-7}$ M.

Although both mechanisms III and IV can account for the pH dependence of the $k_{1\,app}$ data, they are not valid because the principle of detailed balancing is violated. By applying this principle to mechanism III, it can be shown that

$$k_8 = \frac{k_7k_{-8}K_{2c}}{k_{-7}K_2} \quad (13)$$

Using reverse rate constant data from above and other data from Table II in the right side of eq 13, one obtains a detailed balance value of $k_8 = (3.0 \pm 1.6) \times 10^7$ M^{-1} sec^{-1}, while the direct kinetic analysis results in a value of $k_8 \leq 20$ M^{-1} sec^{-1}. Similar analysis applied to mechanism IV results in $k_9 = (3.1 \pm 1.6) \times 10^7$ M^{-1} sec^{-1} compared with $k_9 \leq 1 \times 10^4$ M^{-1} sec^{-1}. In addition, in the case of mechanism IV, evidence from inorganic chemistry indicates that cyanide complexes of transition metals do not exist with HCN as the bound ligand (Jones, 1963; Griffith, 1962). If mechanism IV is revised

so the ligand is bound as the anion, it is not possible to fit the $k_{-1\,app}$ data with the equation derived from this version. Thus mechanisms III and IV must be eliminated.

We finally consider mechanism V which involves three heme-linked ionizable groups:

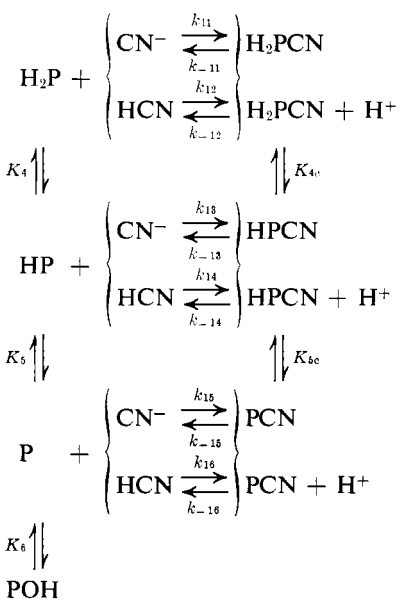

(V)

The corresponding rate equations are

$$k_{1\,app} = \frac{k_{11} + \frac{k_{13}K_4}{(H^+)} + \frac{k_{15}K_4K_5}{(H^+)^2}}{\left(1 + \frac{K_4}{(H^+)} + \frac{K_4K_5}{(H^+)^2} + \frac{K_4K_5K_6}{(H^+)^3}\right)\left(1 + \frac{(H^+)}{K_L}\right)} + \frac{k_{12} + \frac{k_{14}K_4}{(H^+)} + \frac{k_{16}K_4K_5}{(H^+)^2}}{\left(1 + \frac{K_4}{(H^+)} + \frac{K_4K_5}{(H^+)^2} + \frac{K_4K_5K_6}{(H^+)^3}\right)\left(1 + \frac{K_L}{(H^+)}\right)} \quad (14)$$

$$k_{-1\,app} = \frac{\left[k_{-11} + k_{-12}(H^+) + \frac{k_{-13}K_{4c}}{(H^+)} + k_{-14}K_{4c} + \frac{k_{-15}K_{4c}K_{5c}}{(H^+)^2} + \frac{k_{-16}K_{4c}K_{5c}}{(H^+)}\right]}{1 + \frac{K_{4c}}{(H^+)} + \frac{K_{4c}K_{5c}}{(H^+)^2}} \quad (15)$$

Four simplifications of mechanism V and of the corresponding eq 14 and 15 fit the experimental rate data satisfactorily and do not violate the principle of detailed balancing. These simplified versions of mechanism V all contain two pairs of forward and reverse specific rate constant terms. All other terms do not contribute. The forward rate constants for these four simplifications are: (A) k_{11}, k_{13}; (B) k_{14}, k_{16}; (C) k_{13}, k_{14}; and (D) k_{11}, k_{16}. The various kinetic and equilibrium parameters, obtained from nonlinear least-squares analysis, are listed in Table III. The same equilibrium constants for the heme-linked

TABLE III: Rate and Equilibrium Constants of Simplified Versions A–D, respectively, of Mechanism V.

k_{11}	$(7.4 \pm 1.3) \times 10^9\ M^{-1}\ sec^{-1}$	*a*	*a*	*a*	$(7.4 \pm 1.3) \times 10^9\ M^{-1}\ sec^{-1}$
k_{12}	*a*	*a*	*a*	*a*	*a*
k_{13}	$(3.8 \pm 0.4) \times 10^7\ M^{-1}\ sec^{-1}$	*a*	$(3.8 \pm 0.4) \times 10^7\ M^{-1}\ sec^{-1}$	*a*	*a*
k_{14}	*a*	$(1.1 \pm 0.2) \times 10^5\ M^{-1}\ sec^{-1}$	$(1.1 \pm 0.2) \times 10^5\ M^{-1}\ sec^{-1}$	*a*	*a*
k_{15}	*a*	*a*	*a*	*a*	*a*
k_{16}	*a*	$(9.3 \pm 1.0) \times 10^4\ M^{-1}\ sec^{-1}$	*a*	$(9.3 \pm 1.0) \times 10^4\ M^{-1}\ sec^{-1}$	*a*
k_{-11}	$0.17 \pm 0.03\ sec^{-1}$	*a*	*a*	$0.17 \pm 0.03\ sec^{-1}$	*a*
k_{-12}	*a*	*a*	*a*	*a*	*a*
k_{-13}	$0.30 \pm 0.03\ sec^{-1}$	*a*	$0.30 \pm 0.03\ sec^{-1}$	*a*	*a*
k_{-14}	*a*	$(9.4 \pm 1.6) \times 10^5\ M^{-1}\ sec^{-1}$	$(9.4 \pm 1.6) \times 10^5\ M^{-1}\ sec^{-1}$	*a*	*a*
k_{-15}	*a*	*a*	*a*	*a*	*a*
k_{-16}	*a*	$(1.4 \pm 0.1) \times 10^{10}\ M^{-1}\ sec^{-1}$	*a*	$(1.4 \pm 0.1) \times 10^{10}\ M^{-1}\ sec^{-1}$	*a*
K_4	$(7.2 \pm 2.0) \times 10^{-5}$ M	$(7.2 \pm 2.6) \times 10^{-5}$ M	$(7.2 \pm 2.6) \times 10^{-5}$ M	$(7.2 \pm 2.0) \times 10^{-5}$ M	$(7.2 \pm 2.6) \times 10^{-5}$ M
K_5	$(4.3 \pm 0.6) \times 10^{-7}$ M	$(4.3 \pm 4.8) \times 10^{-7}$ M	$(4.3 \pm 0.6) \times 10^{-7}$ M	$(4.3 \pm 4.8) \times 10^{-7}$ M	$(4.3 \pm 4.8) \times 10^{-7}$ M
K_6	$(1.4 \pm 0.4) \times 10^{-11}$ M	$(1.4 \pm 0.4) \times 10^{-11}$ M	$(1.4 \pm 0.4) \times 10^{-11}$ M	$(1.4 \pm 0.4) \times 10^{-11}$ M	$(1.4 \pm 0.4) \times 10^{-11}$ M
K_4	$(1.8 \pm 0.9) \times 10^{-7}$ M	$(1.8 \pm 0.9) \times 10^{-7}$ M	$(1.8 \pm 0.9) \times 10^{-7}$ M	$(1.8 \pm 0.9) \times 10^{-7}$ M	$(1.8 \pm 0.9) \times 10^{-7}$ M
K_{5c}	$(2.1 \pm 0.8) \times 10^{-11}$ M	$(2.1 \pm 0.8) \times 10^{-11}$ M	$(2.1 \pm 0.8) \times 10^{-11}$ M	$(2.1 \pm 0.8) \times 10^{-11}$ M	$(2.1 \pm 0.8) \times 10^{-11}$ M

[a] Signifies a rate constant effectively equal to zero.

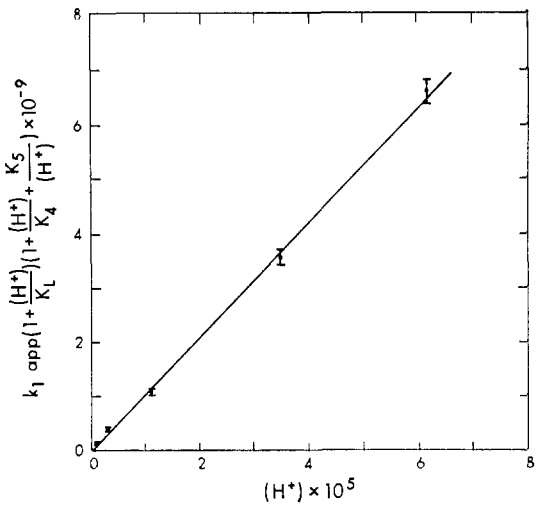

FIGURE 6: Plot of the left side of eq 17 *vs.* (H^+) used to test the validity of mechanism VA for the binding of cyanide by HRP over the pH range 4.2–8.1.

ionizable groups and identical predictions, to four significant figures, of the k_{1app} and k_{-1app} data are obtained from the four mechanisms. The values of k_{1app} and k_{-1app} computed from the best-fit parameters of the four mechanisms are shown by the solid lines in Figures 2 and 3, respectively.

The equivalence of the four mechanisms in their fit to the experimental rate data is a result of symmetry properties inherent in the over-all mechanism V. Thus the rate of binding of CN^- by H_2P, given by $k_{11}(H_2P)(CN^-)$, can be rearranged using the relations $K_4 = (H^+)(HP)/(H_2P)$ and $K_L = (H^+)(CN^-)/(HCN)$ to give $(k_{11}K_L/K_4)\cdot(HP)(HCN)$. Similarly $k_{13}(HP)(CN^-)$ can be converted to $(k_{13}K_L/K_5)(P)(HCN)$. The equivalent fit of mechanisms VA and VB to the experimental kinetic data implies that $k_{14} = k_{11}K_L/K_4$ and $k_{16} = k_{13}K_L/K_5$. These relations are obeyed by the data in Table III. In a similar manner it can be shown from the k_{-1app} data that $k_{-14} = k_{-11}/K_{4c}$ and $k_{-16} = k_{-13}/K_{5c}$. It follows that the four mechanisms, VA–VD, are kinetically indistinguishable. It also follows that appropriate linear combinations of the four mechanisms will provide equally satisfactory fits to the experimental rate data.

As an example of the principle of detailed balancing, it can be shown that

$$k_{13} = \frac{k_{11}k_{-13}K_{4c}}{k_{-11}K_4} \qquad (16)$$

From the values from Table III for the factors in the right side of eq 16, $k_{13} = (3.3 \pm 1.9) \times 10^7\ M^{-1}\ sec^{-1}$ compared to $k_{13} = (3.8 \pm 0.4) \times 10^7\ M^{-1}\ sec^{-1}$ obtained from direct kinetic analysis.

In addition to the four simplified versions of mechanism V discussed above, one other mechanism appears to fit the experimental rate data. It is similar to mechanism VB but involves the formation of a complex with undissociated HCN as the bound form of the ligand. Aside from evidence from inorganic chemistry, it can be eliminated, as was the case with mechanism IV, by applying the principle of detailed balancing.

The predicted pK value for the most acid heme-linked group, 4.1, is consistent with results of other studies (Dunford and Alberty, 1967; Theorell and Paul, 1944). The pK value of 6.4 does not agree with values of 5.0 and 7.0 reported elsewhere (Theorell and Paul, 1944; Harbury, 1957) but is in agreement with a reanalysis of the HRP–fluoride kinetics (see below). The value of this intermediate pK obtained from the HRP–cyanide kinetic data is a sensitive parameter. For example, it is changed from a value of 6.4 to 7.2 by arbitrarily changing the value of pK_L from 9.0 to 9.1. On the other hand the pK's with values of 4.1 and 10.8 are only changed by 0.1 for the same change in pK_L.

The values of the equilibrium constants of the heme-linked groups are shifted to smaller values as a result of the binding of the ligand. This shift is in the direction expected if the bound ligand is negatively charged (Alberty and Massey, 1954).

Large values of k_{11} and k_{-16} are obtained from mechanism V, raising the question of whether these values might exceed the diffusion-controlled limit. An upper limit for a second-order specific rate constant for an enzyme–ligand reaction is of the order of $10^{10}\ M^{-1}\ sec^{-1}$ (Alberty and Hammes, 1958) and, within the error limits of the various parameters required for computing the diffusion-controlled limit, the values of these specific rate constants are not too large.

The four simplifications of eq 14 which fit the experimental data can in turn be simplified in certain pH regions, depending on the relative magnitudes of the various parameters. These simplified equations can be rearranged into linear form to provide an alternative means of calculating some of the parameters, as a check on the nonlinear least-squares analysis. For example, in the pH region 4.21–8.11, the expression for ligand binding according to mechanism VA can be reduced to

$$k_{1app}\left(1+\frac{(H^+)}{K_L}\right)\left(1+\frac{(H^+)}{K_4}+\frac{K_5}{(H^+)}\right) = k_{13}+\frac{k_{11}(H^+)}{K_4} \qquad (17)$$

A plot of the left side of eq 17 *vs.* (H^+) for $K_4 = 7.2 \times 10^{-5}$ M and $K_5 = 4.3 \times 10^{-7}$ M is shown in Figure 6. Linear least-squares analysis of the plot yields the values $k_{11}/K_4 = (1.0 \pm 0.2) \times 10^{14}\ sec^{-1}$ and $k_{13} = (3.6 \pm 0.6) \times 10^7\ M^{-1}\ sec^{-1}$. Similarly, for the pH region 8.55–11.31, eq 14 reduces to

$$k_{1app}\left(1+\frac{(H^+)}{K_L}\right)\left(1+\frac{K_6}{(H^+)}\right)\left(\frac{K_5}{(H)^+}\right) = k_{13} \qquad (18)$$

Using the values $K_5 = 4.3 \times 10^{-7}$ M and $K_6 = 1.4 \times 10^{-11}$ M, calculation of the left side of eq 18 yields a mean value of $k_{13} = (3.9 \pm 0.3) \times 10^7\ M^{-1}\ sec^{-1}$.

In summary, the cyanide kinetic results indicate the presence of three heme-linked groups with pK values of 4.1, 6.4, and 10.8 on horseradish peroxidase. They also

indicate that the anion form of the ligand exists in the ligand–peroxidase complex, but it is impossible to distinguish which, if either, form of the ligand dominates the binding reaction. The same ambiguity exists as to the reactivities of the various peroxidase species.

HRP–Fluoride Kinetics. From the results of a temperature-jump study of the reversible binding of fluoride by HRP (Dunford and Alberty, 1967) it was concluded that the simplest mechanism consistent with the experimental data was

$$\begin{array}{ccc} HP + F^- & \underset{k_{-3}}{\overset{k_3}{\rightleftharpoons}} & HPF \\ K \uparrow\downarrow & & \uparrow\downarrow K_c \\ P + F^- & \underset{k_{-4}}{\overset{k_4}{\rightleftharpoons}} & PF \end{array} \qquad \begin{array}{l} \text{(III)} \\ \text{(fluoride)} \end{array}$$

The nomenclature is identical with that in the original paper. This mechanism can be tested by the principle of detailed balancing, using the relation

$$k_3 = \frac{k_{-3}k_4K}{k_{-4}K_c} \tag{19}$$

The greatest uncertainty occurs in K_c, which can range from 1.0×10^{-6} to 1.3×10^{-5} M according to its nonlinear confidence limits. Using the most favorable value, $K_c = 1.0 \times 10^{-6}$ M, along with $K = 8.8 \times 10^{-5}$ M, $k_{-3} = 2.7 \times 10^2$ sec^{-1}, $k_4 = 3.2 \times 10^2$ M^{-1} sec^{-1}, and $k_{-4} = 4.2 \times 10^2$ sec^{-1}, the detailed balance result is $k_3 = 1.8 \times 10^4$ M^{-1} sec^{-1} compared to $k_3 = 2.0 \times 10^6$ M^{-1} sec^{-1} from direct kinetic analysis.

Therefore the previously published mechanism III appears inadequate. If it is extended to include HF binding, the fit to the experimental data is not improved. From the mechanism

$$\begin{array}{ccc} H_2P + F^- & \underset{k_{-5}}{\overset{k_5}{\rightleftharpoons}} & H_2PF \\ K_1 \uparrow\downarrow & & \uparrow\downarrow K_{1c} \\ HP + F^- & \underset{k_{-6}}{\overset{k_6}{\rightleftharpoons}} & HPF \\ K_2 \uparrow\downarrow & & \uparrow\downarrow K_{2c} \\ P + F^- & \underset{k_{-7}}{\overset{k_7}{\rightleftharpoons}} & PF \end{array} \qquad \begin{array}{l} \text{(IV)} \\ \text{(fluoride)} \end{array}$$

the following equation is obtained

$$k_{1\,app} = \frac{k_5\dfrac{(H^+)}{K_1} + k_6 + k_7\dfrac{K_2}{(H^+)}}{\left(1 + \dfrac{(H^+)}{K_1} + \dfrac{K_2}{(H^+)}\right)\left(1 + \dfrac{(H^+)}{K_L}\right)} \tag{20}$$

Nonlinear least-squares analysis of the $k_{1\,app}$ data yields the results $k_5 = (2.9 \pm 0.5) \times 10^6$, $k_6 = (3.3 \pm 0.7) \times 10^4$, $k_7 = (4.7 \pm 3.0) \times 10^2$, all in M^{-1} sec^{-1}; $K_1 = (4.9 \pm 1.2) \times 10^{-5}$ M and $K_2 = (8.3 \pm 2.0) \times 10^{-7}$ M. Values of $k_{-5} = (2.7 \pm 0.4) \times 10^2$ sec^{-1}, $k_{-6} = (4.2 \pm 0.5) \times 10^2$ sec^{-1}, and $K_{1c} = (7.0 \pm 6.0) \times 10^{-6}$ M are unchanged from their corresponding values in mechanism III. The value of pK_{2c} appears to fall outside the range of experimental pH values so that k_{-7} and K_{2c} cannot be obtained from the $k_{-1\,app}$ data.

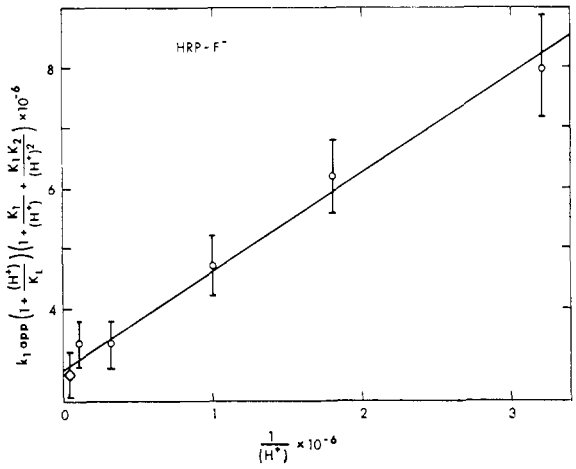

FIGURE 7: Plot of the left side of eq 22 *vs.* $1/(H^+)$ to test the validity of a simplified mechanism IV for the binding of F^- by HRP over the pH range 4.1–6.5. Four points below pH 5.0 are combined into a mean value indicated by ◇. All points were given equal weight in the linear least-squares analysis.

From detailed balancing

$$k_5 = \frac{k_{-5}k_6K_1}{k_{-6}K_{1c}} \tag{21}$$

With the most favorable value of $K_{1c} = 1.0 \times 10^{-6}$ M and the other parameters listed above, eq 21 yields the result $k_5 = 1.0 \times 10^6$ M^{-1} sec^{-1} compared to the kinetic value $k_5 = 2.9 \times 10^6$ M^{-1} sec^{-1}.

The symmetry properties of a mechanism, as applied to the cyanide kinetics, are also of potential application to the HRP–fluoride results. Thus $k_5(H_2P)(F^-)$ can be replaced by a rate expression of the form $k'(HP)(HF)$, and $k_6(HP)(F^-)$ by $k''(P)(HF)$. However, there is no corresponding HF term for $k_7(P)(F^-)$ for the pH range of the study, making improbable any mechanism which assumes that the attacking ligand is only HF.

Equation 20 for the HRP–fluoride binding kinetics can be simplified under certain conditions. For example, it reduces to

$$k_{1\,app}\left(1 + \frac{(H^+)}{K_L}\right)\left(1 + \frac{K_1}{(H^+)} + \frac{K_1K_2}{(H^+)^2}\right) = k_5 + \frac{k_6K_1}{(H^+)} \tag{22}$$

for the pH range 4.1–6.5. A linear plot of the left side of eq 22 *vs.* $1/(H^+)$ is shown in Figure 7. From the intercept $k_5 = (3.0 \pm 0.6) \times 10^6$ M^{-1} sec^{-1} and, using $K_1 = 4.9 \times 10^{-5}$ M, the slope yields $k_6 = (3.3 \pm 0.7) \times 10^4$ M^{-1} sec^{-1}, in excellent agreement with the nonlinear least-squares analysis of eq 20.

Acknowledgments

We thank Mr. Raymond Anderson for valuable technical assistance during this investigation. We also thank Dr. G. G. Hammes at Cornell and the following colleagues at the University of Alberta for helpful comments: Mr. N. S. Angerman, Dr. D. Dolman, and Dr. R. B. Jordan.

References

Alberty, R. A., and Hammes, G. G. (1958), *J. Phys. Chem. 62*, 154.

Alberty, R. A., and Massey, V. (1954), *Biochim. Biophys. Acta 13*, 347.

Chance, B. (1943), *J. Cellular Comp. Physiol. 22*, 33.

Davies, C. W. (1938), *J. Chem. Soc.*, 2093.

Dunford, H. B., and Alberty, R. A. (1967), *Biochemistry 6*, 447.

Frost, A. A., and Pearson, R. G. (1961), Kinetics and Mechanism, 2nd ed, New York, N. Y., Wiley, p 187.

Griffith, W. P. (1962), *Quart. Rev. (London) 16*, 188.

Harbury, H. A. (1957), *J. Biol. Chem. 225*, 1009.

IBM Share Library (1964), Program SDA 3094, modified for use on University of Alberta IBM 360 computer.

Izatt, R. M., Christensen, J. J., Pack, R. T., and Bench, R. (1962), *Inorg. Chem. 1*, 828.

Jones, L. H. (1963), *Inorg. Chem. 2*, 777.

Kay, E., Shannon, L. M., and Lew, J. Y. (1967), *J. Biol. Chem. 242*, 2470.

Keilin, D., and Hartree, E. F. (1951), *Biochem. J. 49*, 88.

King, E. L. (1964), How Chemical Reactions Occur, New York, N. Y., Benjamin, p 131.

Maehly, A. C. (1952), *Biochim. Biophys. Acta 8*, 1.

Shannon, L. M., Kay, E., and Lew, J. Y. (1966), *J. Biol. Chem. 241*, 2166.

Theorell, H. (1942), *Arkiv Kemi. Mineral. Geol. 16A*, No. 3.

Theorell, H., and Paul, K. G. (1944), *Arkiv Kemi. Mineral. Geol. 18A*, No. 12.

Ver Ploeg, D. A., and Alberty, R. A. (1968), *J. Biol. Chem. 243*, 435.